International Journal of Biological Macromolecules 121 (2019) 398–406

Contents lists available at ScienceDirect

International Journal of Biological Macromolecules

journal homepage: http://www.elsevier.com/locate/ijbiomac

Incorporation of magnetic NaX zeolite/DOX into the PLA/chitosan nanofibers for sustained release of doxorubicin against carcinoma cells death in vitro

Payam Abasian [a], Maryam Radmansouri [b], Mania Habibi Jouybari [c], Mina Vaez Ghasemi [d], Ali Mohammadi [e], Mohammad Irani [f,*], Fariborz Sharifian Jazi [g]

[a] Department of Chemical and Petroleum Engineering, Sharif University of Technology, Tehran, Iran
[b] Department of Clinical Biochemistry, School of Pharmacy and Pharmaceutical Sciences, Isfahan Pharmaceutical Sciences Research Centre, Isfahan University of Medical Sciences, Isfahan, Iran
[c] Department of Pharmaceutics, School of Pharmacy, Tehran University of Medical Sciences, Tehran, Iran
[d] Faculty of New Sciences and technologies, Department of Life Science Engineering, University of Tehran, Tehran, Iran
[e] Department of Medicinal Chemistry, Faculty of Pharmacy, Pharmaceutical Sciences Branch, Islamic Azad University, Tehran, Iran
[f] Young Researchers & Elite Club, Tehran North Branch, Islamic Azad University, Tehran, Iran
[g] Young Researchers and Elite Club, Najafabad Branch, Islamic Azad University, Najafabad, Isfahan, Iran

ARTICLE INFO

Article history:
Received 23 July 2018
Received in revised form 4 September 2018
Accepted 28 September 2018
Available online 2 October 2018

Keywords:
NaX Nanozeolites
PLA/chitosan/NaX/Fe_3O_4/DOX
Nanofibers
Anticancer
Carcinoma

ABSTRACT

In the present study, the magnetic NaX nanozeolites were synthesized via microwave heating method and loaded into the PLA/chitosan solution. Doxorubicin (DOX) as an anticancer drug was simultaneously incorporated into the PLA/chitosan solution and the electrospinning process was used to fabricate the PLA/chitosan/NaX/Fe_3O_4/DOX nanofibers for sustained release of DOX against carcinoma cells death. The synthesized nanozeolites were characterized using X-ray diffraction (XRD), field emission scanning electron microscopy (FESEM) and energy dispersive X-ray spectroscopy (EDX) analysis. The scanning electron microscopy (SEM) was used to determine the morphology and fiber diameter distribution of synthesized nanofibers. The DOX loading efficiency and in vitro DOX release profiles from nanofibers were investigated. The kinetic models including zero-order, Higuchi and Korsmeyer-Peppas were used to analyze the release mechanism of DOX from nanofibers. The effect of ferrite nanoparticles on the DOX release from chitosan/PLA/NaX/DOX and chitosan/PLA/NaX/Fe_3O_4/DOX nanofibers have been investigated in the presence of magnetic field and without magnetic field. The antitumor activity of synthesized nanofibers was also investigated on the carcinoma cells death. The maximum killing percentage of H1355 cells was found to be 82% using DOX loaded chitosan/PLA/NaX/ferrite in the presence of external magnetic field after 7 days of treatment.

1. Introduction

The synthetic and natural zeolites due to the low toxicity, good dispersity, and surface functional groups have high efficiency for biomedical applications such as immobilization of enzymes for biosensing, wound treatment, tissue engineering and drug delivery systems [1–5]. The microporous structure of zeolites with cages and channels on a nano- and subnanometer scales provide them for drug delivery [6–9]. The nanozeolites as aluminosilicate crystals due to unique properties such as small size, more ion-exchanged sites, and high chemical stability as well as high adsorption capacity exhibited the higher drug loading efficiency and sustained release of drug [10–15]. The cytotoxicity of nanozeolite is related to its shape, zeolite dosage, size, surface and composition [16–18]. Zeolites have been examined as carriers for loading of variety of drugs. Among synthetic zeolites, zeolite Y has been used for loading Ibuprofen, 5-fluorouracil, aspirin, erythromycin, carbamazepine, and levofloxacin [10,19]. The potential of NaA zeolite was studied for doxorubicin (DOX) loading [7]. Clinoptilolite as a natural zeolite was used for encapsulating erythromycin, aspirin, and sulfamethoxazole [20]. Fisher et al. [21] incorporated the fluorescein diacetate into the MCM-41 and NaX zeolites for the release of drug. However, the nanozeolites are easily carried away by blood flow and disperse to other organs. Furthermore, the agglomeration of nanozeolites is occurred during time. To overcome these problems, the nanozeolites can be incorporated into the polymeric matrix. The nanofibrous scaffolds prepared by electrospinning process due to their high specific area and high porosity with fine pores have a high potential for drug delivery [22–27]. Furthermore, the incorporation of magnetic materials such as ferrite nanoparticles, graphene oxide and multi-walled carbon

* Corresponding author.
E-mail address: irani_mo@ut.ac.ir (M. Irani).

https://doi.org/10.1016/j.ijbiomac.2018.09.215
0141-8130/

nanotubes can increase the treatment effectiveness of drug delivery systems for cancer treatment via targeting of tumor sites and following accumulation of anticancer drugs in the target region [23,25]. Rieger et al. [28] attached the Linde Type A (LTA) zeolites on the surface of the cellulose nanofiber mats. They found that the cellulose/LTA composites were more practical to use in biomedical applications compared with zeolite powders. Takai et al. [29] incorporated the different zeolites into the PVA nanofibers for adsorption of Creatinine. In previous study, we investigated the potential of PVA/NaX composite nanofibers for adsorption of nickel and cadmium from aqueous solutions [30]. Lopes et al. [31] synthesized the PVDF/NaY zeolite-filled nanofibrous scaffolds via electrospinning process. The MC3T3-E1 cells viability results on the composite nanofibers after 72 h of cell culture indicated the suitability of the composite nanofibers for tissue engineering applications. Tran et al. [32] fabricated the electrospun cellulose acetate (CA) fibers/zeolite A nanofibers for lead ions sorption. They found that the incorporating nanozeolites into the nanofibers was an effective method for heavy metal ion removal from water. Anis et al. [33] reviewed the potential of zeolite fibers for catalytic applications. Mehrasa et al. [1] prepared the electrospun zeolite loaded-PVA/collagen nanofibers as a biomimetic platform for chondrocyte cells in tissue engineering. The obtained results revealed that cell proliferations on the PVA/collagen/zeolite nanofibers were higher than that of the pure PVA/collagen nanofibers. Sotoudeh et al. [34] loaded the nanozeolite particles into the PEG/polyacrylic acid/polyacrylamide hydrogel for controlled release of Amoxicillin (antibiotic drug) from composite hydrogel. However, there is a little study on the application of composite nanofibers containing zeolite for controlled release of anticancer drugs.

In the present study, the NaX nanozeolite and DOX were simultaneously incorporated into the PLA/chitosan nanofibers for sustained release of doxorubicin against carcinoma cells death. The synthesized nanozeolites and nanofibers were characterized using X-ray diffraction (XRD), field emission scanning electron microscopy (FESEM) equipped with EDX, and scanning electron microscopy (SEM). The DOX loading efficiency and the in vitro drug release of DOX from nanofibers were investigated. The effect of ferrite nanoparticles on the DOX release was evaluated. The antitumor activity of synthesized nanofibers was also investigated on the carcinoma cells death.

2. Experimental

2.1. Materials

The sodium aluminate ($NaAlO_2$) and silica ($D_{av} = 7$ nm) provided form Sigma-Aldrich and sodium hydroxide (NaOH) purchased from Merck (Darmstadt, Germany) company were applied for the synthesis of NaX zeolite nanoparticles. The chitosan (75–85% deacetylated, average Mw: 200 kDa) and poly(lactic acid) (average Mw: 150 kDa, PLA) supplied by the Sigma-Aldrich, and Trifluoroacetic acid (TFA) obtained from Merck (Darmstadt, Germany) were used for preparation of PLA/chitosan nanofibers. DOX was purchased from Sobhan Pharmaceuticals, Iran.

2.2. Synthesis of NaX zeolite, NaX/ferrite and NaX/ferrite/DOX

The NaX zeolites is synthesized by microwave heating method as described previously [30]. Briefly, sodium aluminate and silica were mixed in water with the molar ratios of 5.5 Na_2O:1.0 Al_2O_3:4.0 SiO_2:190H_2O. Then, the microwave heating was proceeded at 90 °C for 3 h. Finally, the prepared powder was washed with ethanol and deionized water and dried at temperature of 60 °C for 24 h.

To synthesize the NaX/ferrite nanoparticles, 0.5 g of synthesized NaX nanoparticles were dispersed in 20 mL of water in an ultrasonic bath for 30 min. Then, 3.5 g of $FeCl_3 \cdot 6H_2O$ and 0.65 g of $FeCl_2 \cdot 4H_2O$ were added into the mixture under stirring for 2 h. Finally, the NaX/Fe_3O_4 composite solution was dried under vacuum at 60 °C for 24 h to obtain the NaX/ferrite nanoparticles. To prepare the magnetic NaX/DOX, 20 mg of synthesized magnetic nanozeolite was added to 20 mL of the DOX solutions (5, 50 and 100 mgL^{-1}) under stirring for 6 h at 25 °C. The final solution was filtrated and washed with the deionized water and dried at room temperature for 24 h.

2.3. Electrospinning process

The 15 wt% PLA solution was prepared by dissolving 1.5 g PLA in 10 mL TFA under stirring at 50 °C for 6 h. The 5 wt% chitosan solution dissolved in TFA was mixed with PLA solution and stirring was continued for further 6 h to obtain a homogenous solution of PLA/chitosan. To prepare the PLA/chitosan/NaX/ferrite/DOX solutions, the prepared NaX/ferrite/DOX solutions were slowly dispersed to the PLA/chitosan solutions at room temperature and stirring was continued for extra 6 h. The prepared solutions were poured into a 5 mL glass syringe with needle tip of 19-gauge. Then, a high voltage was applied between the needle and collector to produce the PLA/chitosan/NaX/ferrite/DOX nanofibers. A voltage of 20 kV, tip-collector distance of 14 cm, and flow rate of 0.5 mL h^{-1} were used though the electrospinning process for fabrication of nanofibers. The set-up of electrospinning process was provided from the Nanomeghyas Fanavaran Company (Iran).

2.4. Characterization tests

The structure and crystalinity of synthesized magnetic NaX were determined using powder's X-ray diffraction (XRD) patterns at 25 °C on a Philips instrument (X'pert diffractometer using Cu-Karadiation) with a scanning speed of 5 min^{-1}. The morphologies of synthesized nanozeolites and DOX-loaded nanozeolies were determined using

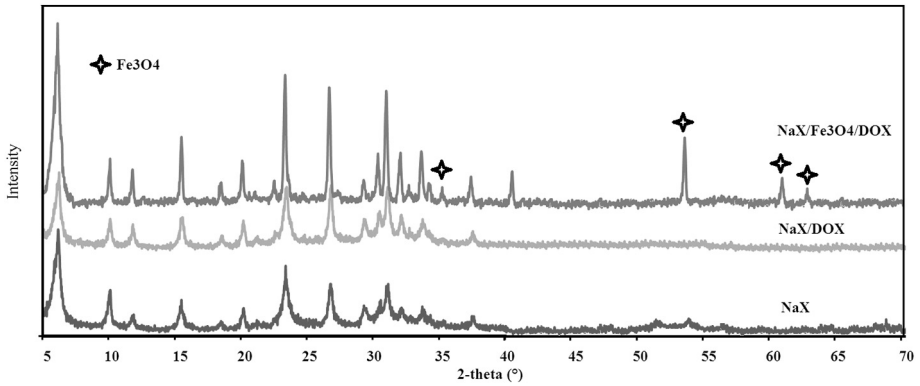

Fig. 1. XRD patterns of NaX zeolite, NaX/DOX and NaX/ferrite/DOX composite.

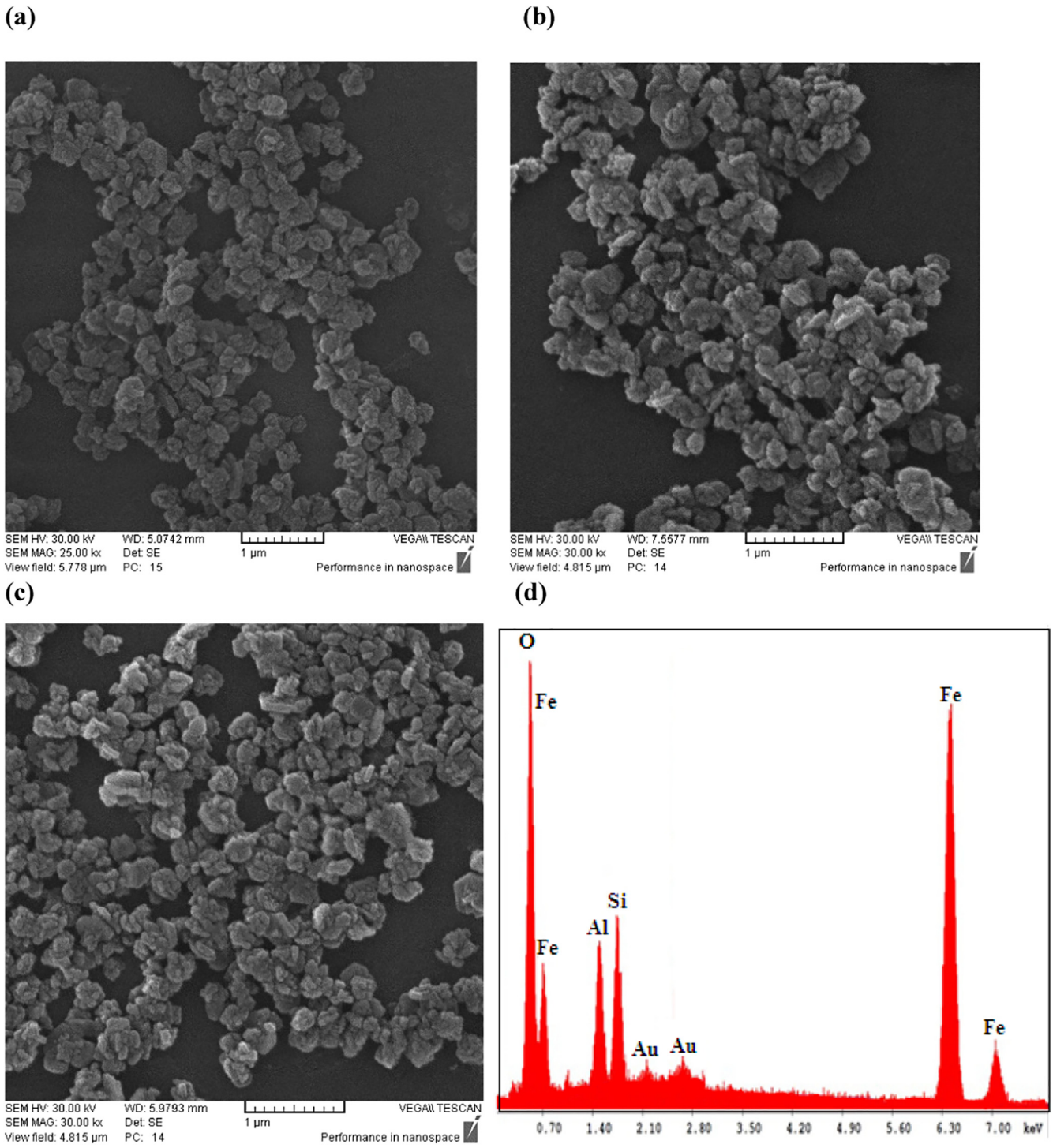

Fig. 2. SEM images of (a) pure NaX zeolite, (b) NaX/DOX, (c) NaX/ferrite/DOX and (d) EDX analysis of NaX/Fe_3O_4.

field emission scanning electron microscopy (MIRA3TESCAN-XMU, FESEM) equipped with energy dispersive X-ray spectroscopy (EDX) after gold coating. The surface morphology and size distribution of the synthesized zeolite and nanofibers were determined using a scanning electron microscopy (SEM, JEOL JSM-6380) after gold coating. The average diameter and diameter distribution of nanofibers were obtained with an image analyzer (Image-Proplus, Media Cybrernetics). The morphology of DOX loaded-PLA/chitosan/NaX/ferrite nanofibers was also investigated using fluorescent microscopy (Evos fl, AMG groups, USA). The drug content in the DOX loaded nanofibers was obtained using an UV–Vis spectrophotometer at a wavelength of 483 nm.

2.5. Drug loading efficiency

To determine the drug loading efficiency, the prepared DOX loaded nanofibers were degraded by dissolving in TFA for 12 h and the final concentration of the drug was measured using UV–Vis

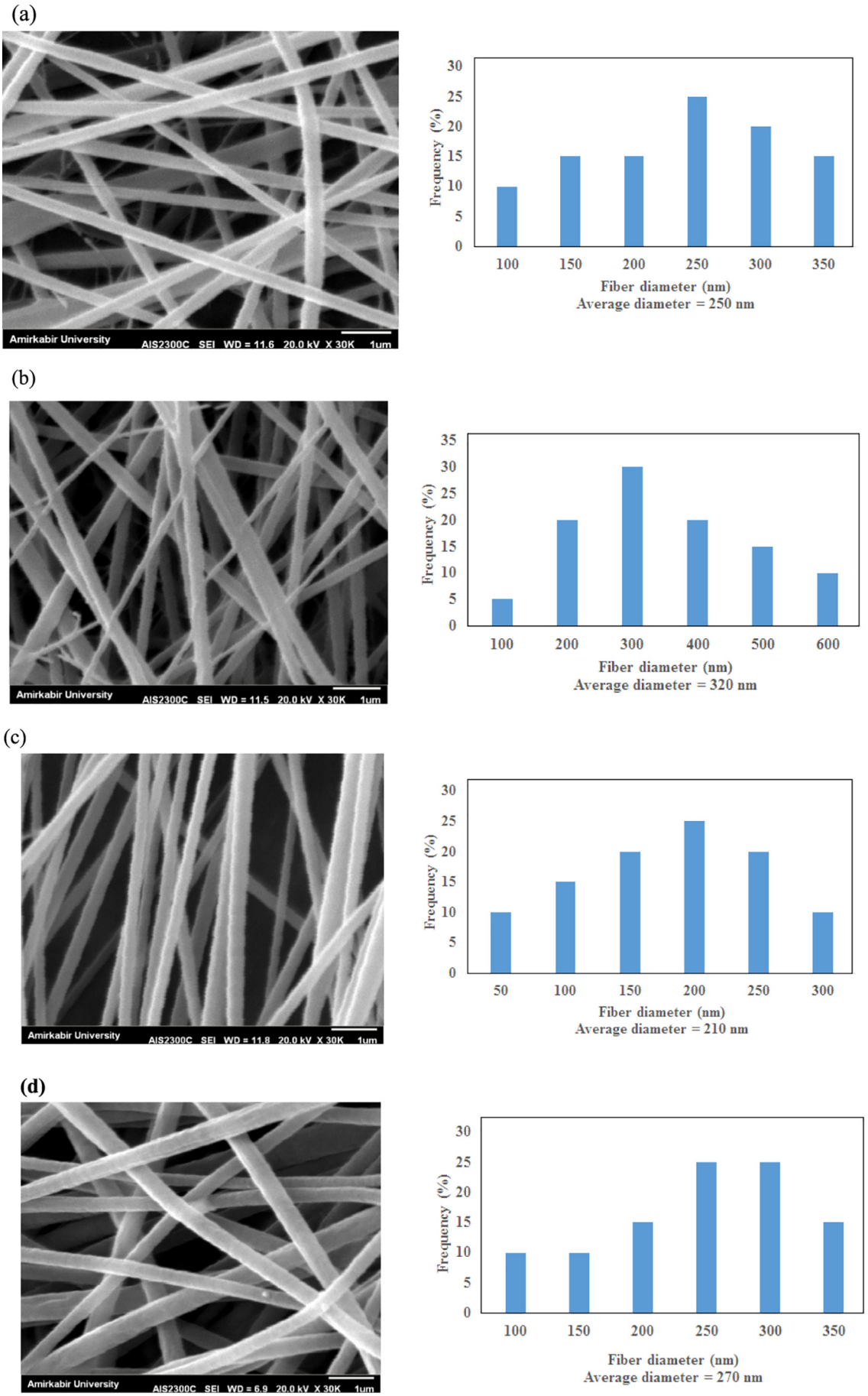

Fig. 3. SEM images of (a) pure chitosan/PLA nanofibers, (b) chitosan/PLA/NaX, (c) chitosan/PLA/NaX/ferrite and (d) chitosan/PLA/NaX/ferrite/DOX nanofibers.

Table 1
Pharmacokinetic parameters for DOX release from prepared nanofibers.

Formulation nanofibers	Zero-order		Higuchi		Korsmeyer-Peppas		
	K_0 (hr^{-1})	R^2	K_H ($hr^{-0.5}$)	R^2	n	K_{KP}	R^2
Chitosan/PLA/DOX	0.0545	0.781	1.312	0.871	0.259	13.42	0.990
Chitosan/PLA/NaX/ferrite/DOX	0.0531	0.731	1.301	0.851	0.244	13.02	0.992

spectrophotometer. The drug loading efficiency (DLE, %) was calculated as follows:

$$\mathrm{DLE}(\%) = \frac{\text{Finaldrug content}}{\text{Drug loading content at the beginning}} \times 100\% \quad (1)$$

2.6. In vitro drug release study and kinetic parameters

The DOX release profiles from the prepared PLA/chitosan/NaX/ferrite/DOX nanofibers were obtained at physiological pH of 7.4 and 37 °C. First, 50 mg of the nanofibers were poured into the 25 mL of Na_2HPO_4–KH_2PO_4 buffer solution with pH of 7.4 at shaking water bath (Hidolff) under stirring of 100 rpm for 30 days. 2 mL of released solutions were taken from the dissolution medium at predetermined intervals, while an equal amount of fresh buffer solutions was added back to the incubation media. The final content of the released DOX in the buffer solution was determined using UV–Vis spectrophotometer. All the drug release experiments were repeated at least three times and the average values were reported.

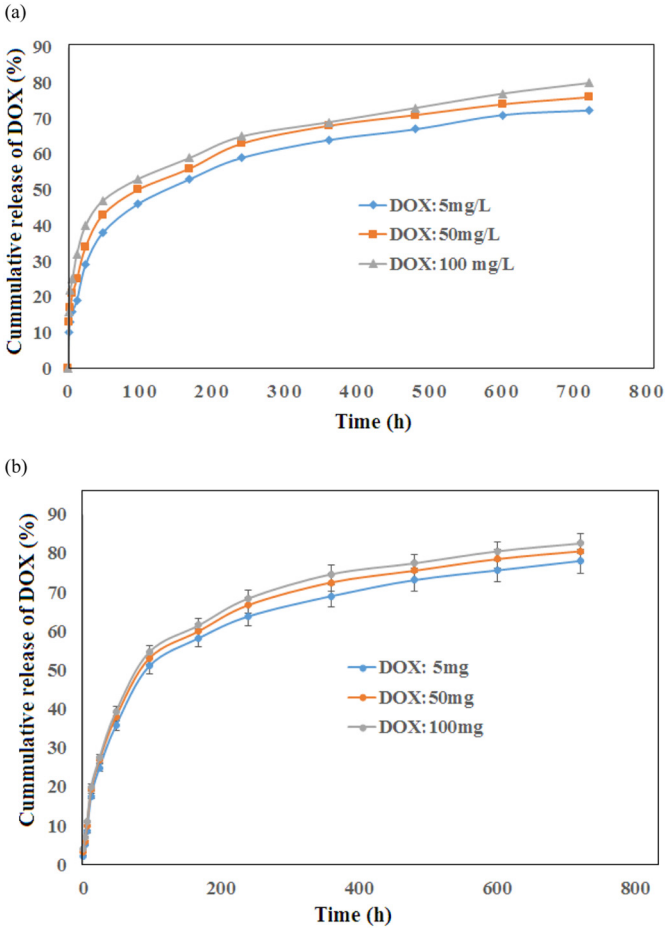

Fig. 4. (a) DOX release from chitosan/PLA/DOX and (b) chitosan/PLA/NaX/DOX nanofibers.

Three pharmacokinetic models including zero-order (Eq. (2)), Higuchi (Eq. (3)) [35] and Korsmeyer-Peppas (Eq. (4)) [36] were used to analyze the release mechanism of DOX from nanofibers. The kinetic parameters were obtained by linear regression using MATLAB software.

$$Q = Q_0 - K_0\, t \quad (2)$$

$$\mathrm{Log}\ Q = \tfrac{1}{2}\ \log t + \log K_H \quad (3)$$

$$\mathrm{Log}\ (M_t/M_\infty) = n \log t + \log K_{KP} \quad (4)$$

where Q_0 and Q are the loaded DOX content and DOX released from nanofibers after time t, respectively. K_0, K_H, and K_{KP} are the constant parameters of Zero-order, Higuchi and Korsmeyer-Peppas equations, respectively. M_t/M_∞ is the fractional release of DOX at time t and '*n*' is the diffusional coefficient related to the release mechanism [36]. When $n < 0.5$, a Fickian diffusion controlled-release is implied; while $0.5 < n < 1.0$ indicates a release non-Fickian and 1 stands for zero order (case II transport). When n value is greater than 1.0, it indicates super case II transport.

2.7. MTT assay

The cell viability MTT (3-(4,5-dimethyl thiazol-2-yl)-2,5-diphenyl tetrazolium bromide, Sigma Aldrich) assay was carried out with H1355 human lung epidermoid carcinoma cell line (cell bank of Pasteur Institute (Tehran, Iran)) to determine the effect of DOX loaded PLA/chitosan/NaX/Fe_3O_4 nanofibers on carcinoma cells death. For the MTT assay, 3×10^4 cells/well were seeded in a 48-well plate and were treated with 50, 100, 250, 500 and 1000 μg/mL concentrations of pristine DOX and equivalent doses of DOX-loaded nanofibers. The plate was incubated in 5% CO2 incubator at 37 °C for 24, 48 and 72 h. Then, 20 μL of MTT solutions were added to each of the wells, and the samples were then incubated for further 4 h. finally, 50 μL of medium were transferred to a 96-well plate and the relative growth inhibition compared with control cells (untreated cells) was determined at wavelength of 570 nm using a ELISA microplate reader (Multiskan MK3, Thermo Electron Corporation, USA). The obtained data were expressed as mean absorbance value (OD) of triplicate samples ± standard deviation of the mean.

3. Results and discussion

3.1. Characterization of zeolite and zeolite/DOX nanoparticles

The XRD patterns of NaX zeolite, NaX/DOX and NaX/ferrite/DOX are illustrated in Fig. 1. For NaX zeolite, the diffraction peaks at 6.12°, 10.91°, 15.35°, 23.21°, 26.94°, 31.94° and 33.24° revealed the synthesized crystals are pure NaX zeolite (JCPDS card no.38–0237). After loading DOX into the NaX zeolite, the framework and the cubic structure of zeolites did not change. However, the intensity and sharpness of the diffraction peaks were slightly decreased which indicated the reduction of crystallinity of DOX-loaded NaX zeolite compared with pure NaX zeolite. The observed diffraction peaks at 35.12°, 41.95°, 54.84°, 62.482° and 63.76° proved the presence of ferrite nanoparticles in the NaX/Fe_3O_4/DOX structure.

The SEM images of pure NaX zeolite, NaX/DOX and NaX/ferrite/DOX are illustrated in Fig. 2. By loading DOX into the NaX, the particles sizes

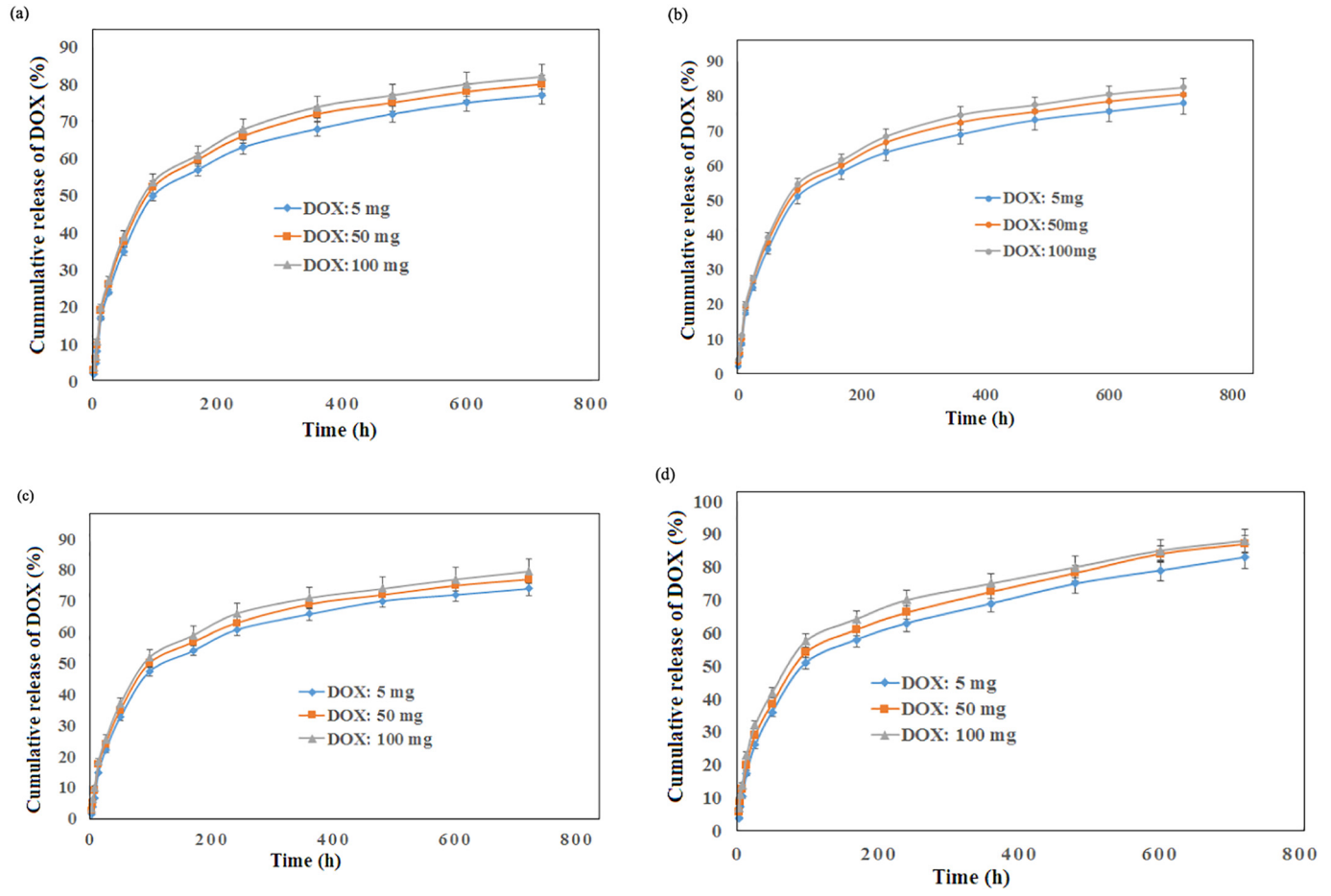

Fig. 5. DOX release from chitosan/PLA/NaX/DOX (a) without external magnetic field and (b) in the presence of magnetic field and DOX release from chitosan/PLA/NaX/ferrite/DOX (c) without external magnetic field and (d) in the presence of magnetic field.

were slightly increased. However, the morphology of particles did not significantly change. This behavior indicated that DOX molecules were successfully incorporated into the zeolite nanoparticles. The comparison of SEM images of NaX and NaX/Fe_3O_4 indicated that the ferrite nanoparticles has not altered the morphology of NaX particles and the crystalline cubic structure of the both NaX and magnetic NaX zeolites were observed. The EDX analysis proved the presence of ferrite nanoparticles into the NaX/Fe_3O_4 composite.

3.2. Characterization of nanofibers

The SEM images of pure chitosan/PLA nanofibers, chitosan/PLA/NaX, chitosan/PLA/NaX/ferrite and chitosan/PLA/NaX/ferrite/DOX and fiber diameter distribution are illustrated in Fig. 3. As shown, by loading NaX particles into the nanofibers, the average diameter of fibers was increased. This behavior indicated that the NaX particles were physically incorporated into the chitosan/PLA nanofibers. The average diameters of chitosan/PLA and, chitosan/PLA/NaX were found to be 250 and 320 nm, respectively. Furthermore, the fiber diameter distribution of chitosan/PLA/NaX was broader than that of chitosan/PLA nanofiber. Also, the reduction of the conductivity of solution and enhancement in the viscosity may be resulted in increasing the fiber diameters of chitosan/PLA/NaX nanofibers. Decrease in the fiber diameter of chitosan/PLA/NaX/ferrite (210 nm) in comparison to chitosan/PLA/NaX nanofibers could be attributed to enhancement in the electrical conductivity of electrospinning precursor solutions. The fiber diameter of chitosan/PLA/NaX/ferrite nanofibers was gradually increased by loading DOX into the nanofibers (240 nm). Furthermore, the surface of nanofibers containing DOX was smooth and no drug crystals were observed, indicating that the drug was finely incorporated into the electrospun fibers.

3.3. Drug loading efficiency

The drug loading efficiencies of DOX-loaded NaX zeolite and chitosan/PLA/NaX/ferrite/DOX nanofibers are presented in Table 1. As can be seen, a high encapsulation efficiency of DOX was observed for both NaX/DOX (97% ± 0.6, 95% ± 0.3 and 96% ± 0.8 for NaX/DOX zeolite containing 5, 50 and 100 mg/L DOX, respectively) and chitosan/PLA/NaX/ferrite/DOX nanofibrous samples (93% ± 0.5, 92% ± 0.2 and 92% ± 0.4 for nanofibers containing 5, 50 and 100 mg/L DOX, respectively). A slightly reduction in DOX encapsulation efficiency of nanofibrous formulations compared with DOX-NaX samples could be attributed to the DOX release from nanofibers surface during electrospinning process.

3.4. DOX release and kinetic studies

The DOX release profiles of chitosan/PLA/DOX and chitosan/PLA/NaX/DOX nanofibers with different drug concentrations (5, 50 and 100 mg) are illustrated in Fig. 4. As shown, the burst release of DOX from chitosan/PLA nanofibers were observed during the first 24 h. However, there are no initial burst releases for DOX release from chitosan/PLA/NaX/DOX nanofibers. The burst release of DOX from chitosan/PLA nanofibers could be attributed to the accumulation of DOX on the surface of nanofibers. The gradual higher burst release of DOX from nanofibers by increasing DOX concentration revealed the accumulation of higher drug molecules near or on the nanofibers surface [37]. The sustained release of DOX from chitosan/PLA/NaX/

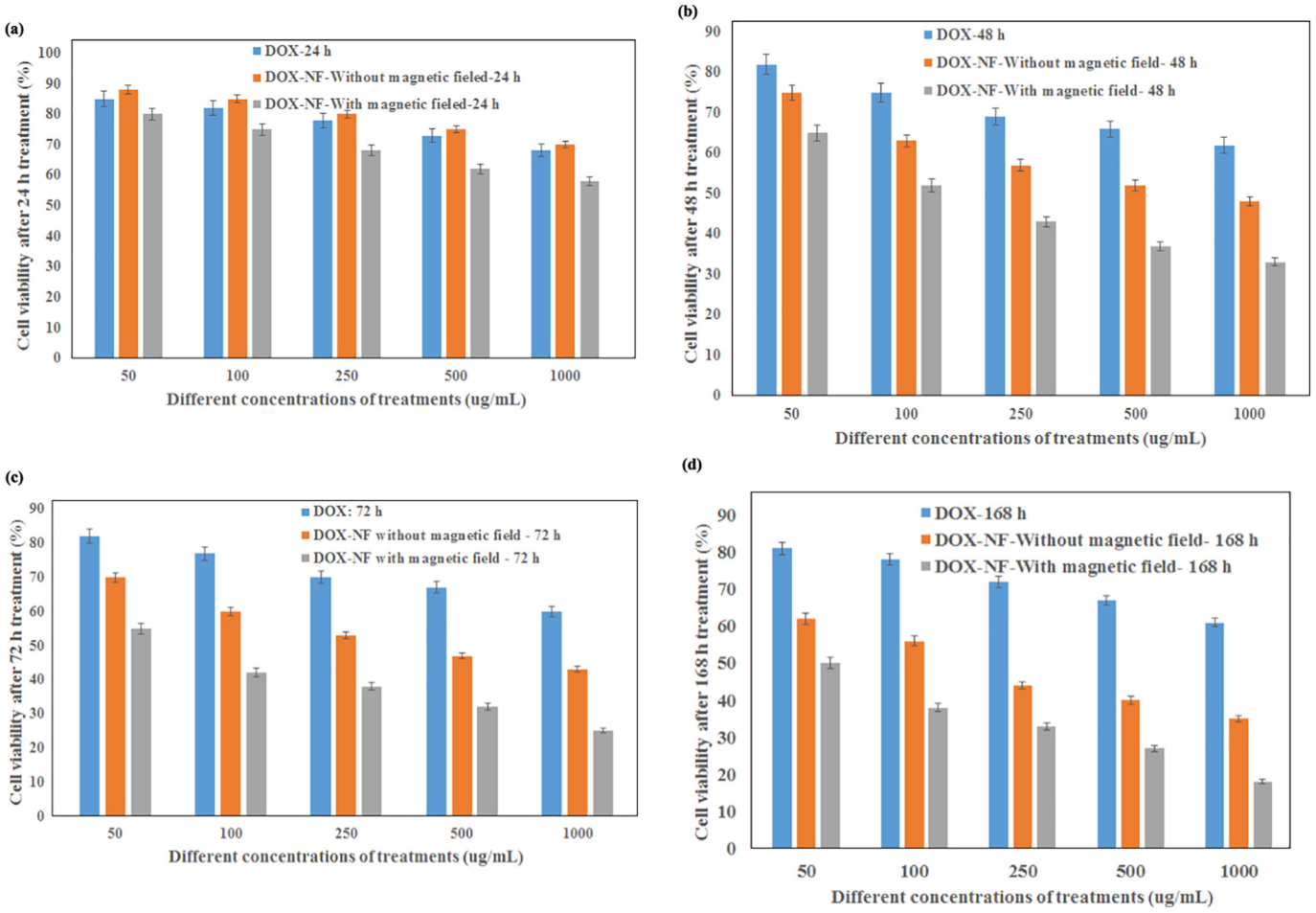

Fig. 6. The cell viability of pristine DOX and DOX loaded nanofibers.

DOX nanofibers without burst release could be attributed to the release of DOX in two stages. The first stage was the DOX release from NaX zeolite and the second stage was the DOX release from pores of nanofibrous scaffold. Also, the release rate was significantly decreased by the drug diffusion from the nanofibers in two stages. The drug release rate was slightly enhanced by increasing DOX concentration in nanofibers.

To investigate the effect of ferrite nanoparticles on the DOX release from nanofibers, the DOX release from chitosan/PLA/NaX/DOX and chitosan/PLA/NaX/ferrite/DOX have been investigated in the presence of magnetic field and without magnetic field which results are illustrated in Fig. 5. As shown, the release rate of DOX from chitosan/PLA/NaX/ferrite/DOX was slightly slower than that of chitosan/PLA/NaX/DOX. This behavior could be attributed to the incorporation of fine pores of nanofibers with ferrite nanoparticles. Furthermore, the release rate of DOX from nanofibers containing ferrite nanoparticles was accelerated in the presence of magnetic field. However, there was no significant change in the DOX release profiles of chitosan/PLA/NaX/DOX by magnetic field and without magnetic field.

The kinetic parameters for DOX release data are presented in Table 1. The Korsmeyer-Peppas release kinetic model was used to describe the DOX release mechanism. When $n \leq 0.5$, a Fickian diffusion controlled-release is implied; while $0.5 < n < 1.0$ indicates a release non-Fickian and 1 stands for zero order (case II transport). When n value is greater than 1.0, it indicates super case II transport. As shown, for both nanofibrous formulations containing various DOX contents, the DOX

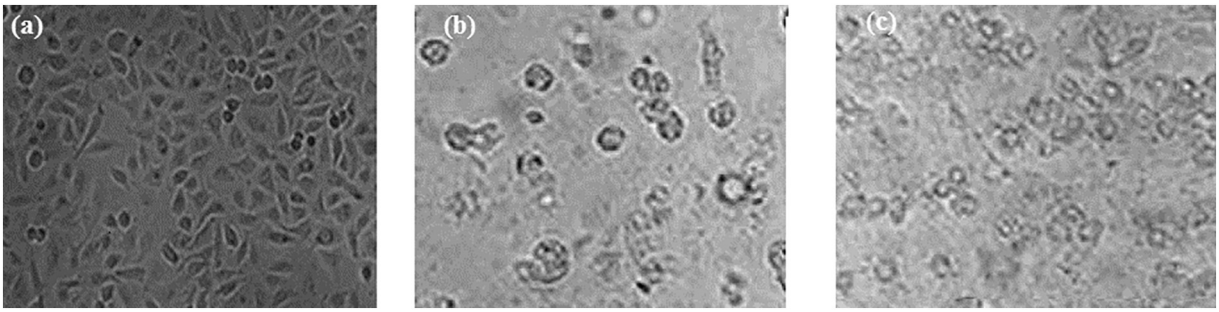

Fig. 7. Photographs of H1355 cancer cells (a) in the presence of PBS as the control, (b) DOX-loaded chitosan/PLA/NaX/ferrite nanofibers and (c) pristine DOX.

release mechanism followed by the Fickian diffusion which indicated that the diffusion of DOX molecules from pores of nanofibers to the PBS solution was the predominant mechanism. Furthermore, the Korsmeyer-Peppas equation was best described the DOX release data compared with zero order and Higuchi kinetic models.

3.5. Cell viability

The results of cell viability against H1355human carcinoma cells are illustrated in Fig. 6.

As shown, the proliferation inhibition effect on target cancer cells was increased by enhancement in concentration of treatments (DOX and DOX loaded nanofibers) in the medium. The maximum killing percentage of H1355 cells was found to be 82% using DOX loaded chitosan/PLA/NaX/ferrite in the presence of external magnetic field after 7 days of treatment. The continuous sustained release of DOX from chitosan/PLA/NaX/ferrite nanofibers and an enhancement in the concentration of the drug at the target site via an external magnetic field could be responsible for the maximum H1355 cells death after 7 days compared to pristine DOX and DOX loaded nanofibers without magnetic field. The lower cytotoxicity of DOX loaded nanofibers without magnetic field against H1355 cells in comparison to pristine DOX after 1 days treatment could be attributed to lower DOX concentration in the medium of the composite nanofibers through the sustained release of DOX from nanofibers. Therefore, the simultaneous use of zeolite and nanofibers for sustained release of anticancer drugs as well as presence of magnetic nanoparticles under an external magnetic field in the drug carrier formulation can improve the effectiveness of chemotherapy and reduce the toxic side effects of anticancer drugs.

The photographs of morphological changes for H1355 cancer cells, DOX-loaded chitosan/PLA/NaX/ferrite nanofibers and pristine DOX are illustrated in Fig. 7. The more inhibition of cancer cells was observed by DOX loaded naanofibers. Furthermore, the.

DOX-loaded nanofibers indicated a higher cytotoxicity compared to pristine DOX. Also, some shrinkages were observed by treatment of cancer cells with pristine DOX. However, the morphology of cancer cells treated with DOX -loaded nanofibers did not significantly change.

4. Conclusion

In this study, the NaX/Fe_3O_4 and DOX were successfully incorporated into the PLA/chitosan nanofibers. The XRD patterns revealed the crystalline structure of NaX and NaX/Fe_3O_4 nanoparticles. The homogenous chitosan/PLA/NaX/ferrite/DOX nanofibers with average diameters of 270 nm were fabricated under applied voltage of 20 kV, tip-collector distance of 14 cm, and flow rate of 0.5 mL h^{-1}. The drug loading efficiencies higher than 90% were observed for DOX-loaded chitosan/PLA/NaX/ferrite nanofibers. The kinetic studies indicated that the DOX release mechanism from nanofibers followed by the Fickian diffusion. The continuous sustained release of DOX and magnetic field effect on the cell viability against H1355 human carcinoma cells resulted in the maximum killing percentage of 82% H1355 cells using DOX loaded chitosan/PLA/NaX/ferrite after 7 days. The obtained results revealed the higher potential of DOX-loaded chitosan/PLA/NaX/ferrite nanofibers in the local chemotherapy of carcinoma tumors.

in the presence of magnetic field and without magnetic field against H1355 human carcinoma cells after (a) 24 h, (b) 48 h and (c) 72 h.

References

[1] M. Mehrasa, A.O. Anarkoli, M. Rafienia, N. Ghasemi, N. Davary, S. Bonakdar, M. Naeimi, M. Agheb, M.R. Salamat, Incorporation of zeolite and silica nanoparticles into electrospun PVA/collagen nanofibrous scaffolds: the influence on the physical, chemical properties and cell behavior, Int. J. Polym. Mater. 65 (2016) 457–465.

[2] T. Kihara, Y. Zhang, Y. Hu, Q. Mao, Y. Tang, J. Miyake, Effect of composition, morphology and size of nanozeolite on its in vitro cytotoxicity, J Biosci Bioeng J 111 (2011) 725–730.

[3] M. Zaarour, M.B. Dong, I. Naydenova, R. Retoux, S. Mintova, Progress in zeolite synthesis promotes advanced applications, Micropor. Mesopor. Mater. 189 (2014) 11–21.

[4] J. Cao, Y. Hu, C. Shen, J. Yao, L. Wei, F. Yang, A. Nie, H. Wang, H. Shen, Y. Liu, Y. Zhang, Nanozeolite-driven approach for enrichment of secretory proteins in human hepatocellular carcinoma cells, Proteomics 9 (21) (2009) 4881–4888.

[5] A. Ricardo, N. Vilaça, O. Martinho, R.M. Reis, M. Sardo, J. Rocha, A.M. Fonseca, F. Baltazar, I.C. Neves, Zeolite structures loading with an anticancer compound as drug delivery systems, J. Phys. Chem. C 116 (2012) 25642–25650.

[6] A. Martucci, L. Pasti, N. Marchetti, A. Cavazzini, F. Dondi, A. Alberti, Adsorption of pharmaceuticals from aqueous solutions on synthetic zeolites, Micropor. Mesopor. Mater. 148 (2012) 174–183.

[7] B. Divband, M.R. Rashidi, M. Khatamian, G.R. Kazemi Eslamian, N. Gharehaghaji, F. Dabaghi Tabriz, Linde type A and nano-magnetite/NaA zeolites: cytotoxicity and doxorubicin loading efficiency, Open Chemistry 16 (2018) 21–28.

[8] M.G. Rimoli, M.R. Rabaioli, D. Melisi, A. Curcio, S. Mondello, R. Mirabelli, E. Abignente, Synthetic zeolites as a new tool for drug delivery, J. Biomed. Mater. Res. A 87 (2008) 156–164.

[9] A. Dyer, S. Morgan, P. Wells, C. Williams, The use of zeolites as slow release anthelmintic carriers, J. Helminthol. 74 (2000) 137–141.

[10] A. Datt, D. Fields, S.C. Larsen, An experimental and computational study of the loading and release of aspirin from zeolite HY, J. Physic. Chem. C 116 (2012) 21382–21390.

[11] D.G. Fatouros, D. Douroumis, V. Nikolakis, S. Ntais, A.M. Moschovi, V. Trivedi, B. Khima, M. Roldo, H. Nazar, P.A. Cox, In vitro and in silico investigations of drug delivery via zeolite BEA, J. Mater. Chem. 21 (2011) 7789–7794.

[12] M. Spanakis, N. Bouropoulos, D. Theodoropoulos, L. Sygellou, S. Ewart, A.M. Moschovi, A. Siokou, I. Niopas, K. Kachrimanis, V. Nikolakis, P.A. Cox, Controlled release of 5-fluorouracil from microporous zeolites, Nanomed. Nanotechnol, Biology. Med. 10 (2014) 197–205.

[13] B.Y. Deng, C. Deng, D. Qi, C. Liu, J. Liu, X. Zhang, D. Zhao, Synthesis of core/shell colloidal magnetic zeolite microspheres for the immobilization of trypsin, Adv. Mater. 21 (2009) 1377–1382.

[14] A. Datt, E.A. Burns, N.A. Dhuna, S.C. Larsen, Loading and release of 5-fluorouracil from HY zeolites with varying SiO_2/Al_2O_3 ratios, Micropor. Mesopor. Mater. 167 (2013) 182–187.

[15] M. Arruebo, R. Fernandez-Pacheco, S. Irusta, J. Arbiol, M.R. Ibarra, J. Santamar, Sustained release of doxorubicin from zeolite–magnetite nanocomposites prepared by mechanical activation, Nanotechnology 17 (2006) 4057–4064.

[16] I. Braschi, G. Gatti, G. Paul, C.E. Gessa, M. Cossi, L. Marchese, Sulfonamide antibiotics embedded in high silica zeolite y: a combined experimental and theoretical study of host–guest and guest–guest interactions, Langmuir 26 (2010) 9524–9532.

[17] S. Grund, T. Doussineau, D. Fischer, G.J. Mohr, Mitoxantrone-loaded zeolite beta nanoparticles: preparation, physico-chemical characterization and biological evaluation, J. Colloid Interface Sci. 365 (2012) 33–40.

[18] N. Vilaça, R. Amorim, O. Martinho, R.M. Reis, F. Baltazar, A.M. Fonseca, I.C. Neves, Encapsulation of α-cyano-4-hydroxycinnamic acid into a NaY zeolite, J. Mater. Sci. 46 (2011) 7511.

[19] P. Horcajada, C. Márquez-Alvarez, A. Rámila, J. Pérez-Pariente, M. Vallet-Regí, Controlled release of ibuprofen from dealuminated faujasites, Solid State Sci. 8 (2006) 1459–1465.

[20] A. Rivera, T. Farias, Clinoptilolite–surfactant composites as drug support: a new potential application, Micropor. Mesopor. Mater. 80 (2005) 337–346.

[21] K.A. Fisher, K.D. Huddersman, M.J. Taylor, Comparison of micro-and mesoporous inorganic materials in the uptake and release of the drug model fluorescein and its analogues, Chem. Eur. J. 9 (2003) 5873–5878.

[22] M. Radmansouri, E. Bahmani, E. Sarikhani, K. Rahmani, F. Sharifianjazi, M. Irani, Doxorubicin hydrochloride-loaded electrospun chitosan/cobalt ferrite/titanium oxide nanofibers for hyperthermic tumor cell treatment and controlled drug release, Int. J. Biol. Macromol. 116 (2018) 378–384.

[23] S. Samadi, M. Moradkhani, H. Beheshti, M. Irani, M. Aliabadi, Fabrication of chitosan/poly(lactic acid)/graphene oxide/TiO2 composite nanofibrous scaffolds for sustained delivery of doxorubicin and treatment of lung cancer, Int. J. Biol. Macromol. 110 (2018) 416–424.

[24] M. Irani, G. Mir Mohamad Sadeghi, I. Haririan, The sustained delivery of temozolomide from electrospun PCL-diol-b-PU/gold nanocompsite nanofibers to treat glioblastoma tumors, Mater. Sci. Eng. C 75 (2017) 165–174.

[25] L. Hosseini, K. Mahboobnia, M. Irani, Fabrication of PLA/MWCNT/Fe_3O_4 composite nanofibers for leukemia cancer cells, Int. J. Polym. Mater. 65 (2016) 176–182.

[26] M. Irani, G. Mir Mohamad Sadeghi, I. Haririan, Gold coated poly(ε-caprolactonediol) based polyurethane nanofibers for controlled release of temozolomide, Biomed. Pharmacother. 88 (2017) 667–676.

[27] M. Irani, G. Mir Mohamad Sadeghi, I. Haririan, A novel biocompatible drug delivery system of chitosan/temozolomide nanoparticles loaded PCL-PU nanofibers for sustained delivery of temozolomide, Int. J. Biol. Macromol. 97 (2017) 744–751.

[28] K.A. Rieger, H.J. Cho, H.F. Yeung, W. Fan, J.D. Schiffman, Antimicrobial activity of silver ions released from zeolites immobilized on cellulose nanofiber mats, ACS Appl. Mater. Interfaces 8 (2016) 3032–3040.

[29] R. Takai, R. Kurimoto, Y. Nakagawa, Y. Kotsuchibashi, K. Namekawa, M. Ebara, Towards a rational design of zeolite-polymer composite nanofibers for efficient adsorption of creatinine, J. Nanomater. 2016 (2016).

[30] L. Roshanfekr Rad, A. Momeni, B. Farshi Ghazani, M. Irani, M. Mahmoudi, B. Noghreh, Removal of Ni^{2+} and Cd^{2+} ions from aqueous solutions using electrospun PVA/zeolite nanofibrous adsorbent, Chem. Eng. J. 256 (2014) 119–127.

[31] A.C. Lopes, C. Ribeiro, V. Sencadas, G. Botelho, S. Lanceros-Méndez, Effect of filler content on morphology and physical–chemical characteristics of poly(vinylidene fluoride)/NaY zeolite-filled membranes, J. Mater. Sci. 49 (9) (2014) 3361–3370.

[32] D.N. Tran, A.M. Marti, K.J. Balkus, Electrospun zeolite/cellulose acetate fibers for ion exchange of Pb^{2+}, Fibers 2 (2014) 308–317.
[33] S.F. Anis, A. Khalil, G. Singaravel, R. Hashaikeh, A review on the fabrication of zeolite and mesoporous inorganic nanofibers formation for catalytic applications, Micropor. Mesopor. Mater. 236 (2016) 176–192.
[34] S. Sotoudeh, A. Barati, R. Davarnejad, M. Aliabadi Farahani, Antibiotic release process from hydrogel nano-zeolite composites, Middle-East J. Sci. Res. 12 (2012) 392–396.
[35] T. Higuchi, Mechanism of sustained action medication. Theoretical analysis of rate of release of solid drugs dispersed in solid matrices, J. Pharm. Sci. 52 (1963) 1145–1149.
[36] R.W. Korsmeyer, R. Gurny, E. Doelker, P. Buri, N.A. Peppas, Mechanisms of solute release from porous hydrophilic polymers, Int. J. Pharm. 15 (1983) 25–35.
[37] A. Sohrabi, P.M. Shaibani, H. Etayash, K. Kaur, T. Thundat, Sustained drug release and antibacterial activity of ampicillin incorporated poly(methyl methacrylate)enylon6 core/shell nanofibers, Polymer 54 (2013) 2699–2705.